

Nanoscale Mapping of the Elasticity of Microbial Cells by Atomic Force Microscopy

Ahmed Touhami,[†] Bernard Nysten,^{‡,§} and Yves F. Dufrêne^{*,†,‡}

Research Center in Micro and Nanoscopic Materials and Electronic Devices and Unité de chimie des interfaces, Université catholique de Louvain, Croix du Sud 2/18, B-1348 Louvain-la-Neuve, Belgium, and Unité de physique et de chimie des hauts polymères, Université catholique de Louvain, Croix du Sud 1, B-1348 Louvain-la-Neuve, Belgium

Received January 27, 2003. In Final Form: April 12, 2003

Single microbial cells can show important local variations of elasticity due to the complex, anisotropic composition of their walls. An example of this is the yeast during cell division, where chitin is known to accumulate in the localized region of the cell wall involved in budding. We used atomic force microscopy (AFM) to measure quantitatively the local mechanical properties of hydrated yeast cells. Topographic images and spatially resolved force maps revealed significant lateral variations of elasticity across the cell surface, the bud scar region being significantly stiffer than the surrounding cell wall. To get quantitative information on sample elasticity, force curves were converted into force vs indentation curves. The curves were then fitted with the Hertz model, yielding Young's modulus values of 6.1 ± 2.4 and 0.6 ± 0.4 MPa for the bud scar and surrounding cell surface, respectively. These data lead us to conclude that in yeast, the bud scar is 10 times stiffer than the surrounding cell wall, a finding which is consistent with the accumulation of chitin in the bud scar region. This is the first report in which spatially resolved AFM force curves are used to distinguish regions of different elasticity at the surface of single microbial cells in relation with function (i.e., cell division). In future research, this approach will provide fundamental insights into the spatial distribution of physical properties at heterogeneous microbial cell surfaces.

Introduction

Unlike animal cells, microbial cells are surrounded by thick, mechanically strong cell walls which determine cellular shape and enable the organisms to resist turgor pressure. The cell wall mechanical properties also play important roles in controlling cell growth and division processes. During the past decades, much progress has been made in understanding the surface properties of microorganisms. Yet physical properties remain difficult to address at the subcellular level due to the small size of the cells. In this context, atomic force microscopy (AFM) has recently emerged as a valuable tool.¹ AFM can be used not only to image the sample surface topography at high resolution² but also to locally measure the elastic properties of materials using it as a nanoindentation technique.^{3–9} To this end, force curves are recorded and converted into force vs indentation curves using appropriate treatments. The curves can then be analyzed with theoretical models to provide quantitative information on sample elasticity (i.e., Young's modulus). This nano-

indentation method enabled the measurement of the mechanical properties of animal cells, including glial cells, platelets, cardiomyocytes, macrophages, endothelial cells, epithelial cells, fibroblasts, and osteoblasts, in relation with various dynamic processes.^{4,5,7–9} Concerning plant cells, Callow et al.¹⁰ determined the Young's modulus of a green plant cell adhesive glycoprotein to be 0.5 MPa and showed that within minutes of release the adhesive underwent a progressive curing process reflected in a 10-fold increase in stiffness. AFM force measurements have also been applied to microbial specimens. For isolated sheaths of the archeon *Methanospirillum hungatei* GP1, the "depression technique", which is complementary to the indentation method, yielded an elastic modulus of 20–40 GPa, indicating this single-layered structure of unusual strength could withstand an internal pressure of 400 atm.¹¹ For isolated murein sacculi of Gram-negative bacteria in the hydrated state, elastic moduli of 25 MPa were measured, in excellent agreement with theoretical calculation of the elasticity of the peptidoglycan network.¹² With the nanoindentation approach, the wall compressibility of whole *Magnetospirillum gryphiswaldense* cells was determined to be about 42 mN/m¹³ and the turgor pressure was determined to be in the range of 85–150 kPa.¹⁴ To our knowledge, the application of spatially resolved AFM force curves to quantitatively distinguish regions of different elasticity on single microbial cells has not been reported.

Microorganisms can show important lateral variations of surface properties (i.e., topography, physicochemical

* To whom correspondence may be addressed. Phone: (32) 10 47 36 00. Fax: (32) 10 47 20 05. E-mail: dufrene@cifa.ucl.ac.be.

[†] Unité de chimie des interfaces.

[‡] Research Center in Micro and Nanoscopic Materials and Electronic Devices.

[§] Unité de physique et de chimie des hauts polymères.

(1) Dufrêne, Y. F. *J. Bacteriol.* **2002**, *184*, 5205.

(2) Binnig, G.; Quate, C. F.; Gerber, C. *Phys. Rev. Lett.* **1986**, *56*, 930.

(3) Burnham, N. A.; Colton, R. J. *J. Vac. Sci. Technol., A* **1989**, *7*, 2906.

(4) Weisenhorn, A. L.; Khorsandi, M.; Kasas, S.; Gotzos, V.; Butt, H.-J. *Nanotechnology* **1993**, *4*, 106.

(5) Radmacher, M.; Fritz, M.; Kacher, C. M.; Cleveland, J. P.; Hansma, P. K. *Biophys. J.* **1996**, *70*, 556.

(6) Tomasetti, E.; Legras, R.; Nysten, B. *Nanotechnology* **1998**, *9*, 305.

(7) Rotsch, C.; Jacobson, K.; Radmacher, M. *Proc. Natl. Acad. Sci. U.S.A.* **1999**, *96*, 921.

(8) Matzke, R.; Jacobson, K.; Radmacher, M. *Nat. Cell Biol.* **2001**, *3*, 607.

(9) Radmacher, M. *Methods Cell Biol.* **2002**, *68*, 67.

(10) Callow, J. A.; Crawford, S. A.; Higgins, M. J.; Mulvaney, P.; Wetherbee, R. *Planta* **2000**, *56*, 641.

(11) Xu, W.; Mulhern, P. J.; Blackford, B. L.; Jericho, M. H.; Firtel, M.; Beveridge, T. J. *J. Bacteriol.* **1996**, *178*, 3106.

(12) Yao X.; Jericho, M.; Pink, D.; Beveridge, T. *J. Bacteriol.* **1999**, *181*, 6865.

(13) Arnoldi, M.; Kacher, C. M.; Bäuerlein, E.; Radmacher, M.; Fritz, M. *Appl. Phys. A: Matter. Sci. Process.* **1998**, *66*, S613.

(14) Arnoldi, M.; Fritz, M.; Bäuerlein, E.; Radmacher, M.; Sackmann, E.; Boulbitch, A. *Phys. Rev. E* **2000**, *62*, 1034.

properties, and elasticity) due to the anisotropic composition of their cell walls. An example of this is the yeast *Saccharomyces cerevisiae* during the course of the division process. The yeast cell wall consists essentially of a microfibrillar array of β 1–3 glucans overlaid by an outer layer of β 1–6 glucans and mannoproteins.¹⁵ Just before bud emergence, a ring of chitin is formed in the cell wall. This ring remains at the base of the bud as the bud grows and ultimately forms part of the bud scar marking the division site on the mother cell.^{16,17} Chitin is a polysaccharide of (β 1–4)-linked *N*-acetylglucosamine, which serves to strengthen the supporting structures of various organisms. In *S. cerevisiae*, chitin is thought to play an essential role in stiffening the localized region of the cell wall involved in budding but a direct, quantitative demonstration of this effect is still lacking. To address this issue, we mapped the surface elasticity of *S. cerevisiae* cells in aqueous solution, using spatially resolved AFM force measurements. Treatment of the force vs indentation curves with the Hertz model shows that the cell wall Young's modulus varies significantly across the cell surface, the bud scar being about 10 times stiffer than the surrounding cell wall.

Materials and Methods

The brewer's yeast strain *Saccharomyces cerevisiae* MUC138475 (top fermenting) was kindly supplied by Professor A. M. Corbisier (Unité de Microbiologie, Université catholique de Louvain, Belgium). The cells were grown as described by Dengis et al.¹⁸ Yeast cells were stored in 25% (vol/vol) glycerol at -20 °C. They were plated in Petri dish on solid medium (1% (wt/vol) yeast extract, 3% (wt/vol) glucose, 2.5% (wt/vol) agar) and incubated at 30 °C for 3 days. The plates were stored at 4 °C and repitched every 3 weeks by plating one yeast colony on a new solid medium. The culture broth contained 2% (wt/vol) yeast extract and 5% (wt/vol) glucose. Two or three colonies from the solid medium plate were used as inoculum for a 10 mL preculture which was grown by shaking overnight at 30 °C. Then cells of the preculture were used to inoculate 200 mL of culture medium to a concentration of about 2×10^6 cells per mL. The culture was incubated on a shaker at 100 rpm and 30 °C. Cells of the exponential growth phase were harvested after 10 h, washed three times with milliQ water, resuspended in water, and immediately used.

AFM images and force–distance curves were obtained at room temperature, using a commercial microscope (Nanoscope III, Digital Instruments, Santa Barbara, CA). Cells were immobilized by mechanical trapping in polycarbonate membranes (Millipore) with pore size similar to the cell size.¹ After a cell suspension was filtered, the filter was carefully cut (1 cm \times 1 cm), turned upside down, and attached to a steel sample puck (Digital Instruments, Santa Barbara, CA) using a small piece of adhesive tape and the mounted sample was immediately transferred into the AFM liquid cell. All measurements were performed in milliQ water with commercial oxide sharpened Si_3N_4 cantilevers (ThermoMicroscopes, Sunnyvale, CA) with a tip radius of ~ 20 nm. The spring constants of the cantilevers from the used batch were found to be 8 ± 0.4 mN/m, as determined by measuring the free resonance frequency in air.¹⁹ Force curves were recorded at rate of 0.5 $\mu\text{m/s}$ (piezo displacement). Freshly cleaved mica was used as a hard non-deformable substrate for photodetectors sensitivity calibration. The treatment of the experimental deflection vs height curves, their transformation into load vs indentation depth curves, and their fit with theoretical relations were performed

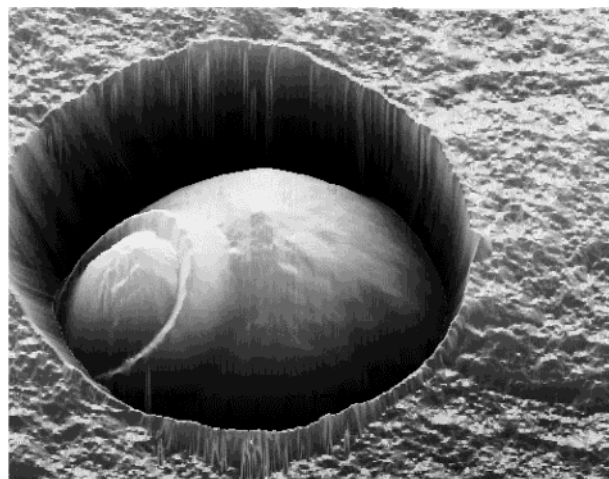


Figure 1. Three-dimensional AFM height image (6 $\mu\text{m} \times 6 \mu\text{m}$; z-range 1 μm), in aqueous solution, showing a single *Saccharomyces cerevisiae* cell protruding from a porous membrane. The cell clearly shows a circular bud scar left after detachment of the daughter cell.

with home-developed routines on Igor Pro software (Wavemetrics Inc., Lake Oswego, OR). Mean values of the Young's modulus were obtained by fitting nine retraction load indentation curves obtained from two independent experiments (different AFM tips, independent cell cultures).

Results and Discussion

Mapping Cell Surface Properties. Single *S. cerevisiae* cells were immobilized in porous polymer membranes. Figure 1 presents a three-dimensional height image of a cell trapped into a pore of the membrane. The cell showed an heterogeneous morphology, the presence of a circular depression being clearly observed. This surface heterogeneity may be attributed to the bud scar resulting from the cell division process, in agreement with earlier AFM²⁰ and electron microscopy²¹ observations. High-resolution height and deflection images of the bud scar are shown in parts a and b of Figure 2.²²

To investigate the mechanical properties of the cell wall at various locations, force–volume images²³ consisting of arrays of 32 \times 32 force curves were recorded in parallel with topographic images. For each force curve, the sample vertical displacement, z , was controlled to obtain the same maximum vertical deflection, d , and thus the same maximum applied force (Figure 2d). Then, force maps reflecting qualitatively the sample mechanical properties were generated by taking a slice of the force volume at a given sample height in the contact region of the curves (Figure 2c,d). The obtained force map, shown in Figure 2c, displayed heterogeneous contrast which was correlated with the heterogeneous surface morphology (Figure 2a,b). The bud scar region clearly showed darker contrast compared to the surrounding cell surface, reflecting a difference in deflection on the two regions for the same sample height (Figure 2d). This observation suggests that the bud scar is qualitatively stiffer than the mother cell wall.

Force vs Indentation Curves. To quantitatively assess the elasticity of the bud scar and mother cell wall

(15) Fleet, G. H. In *The yeasts: yeast organelles*; Rose, A. H., Harrison, J. S., Eds.; Academic Press: London, 1991; p 199.

(16) DeMarini, D. J.; Adams, A. E. M.; Fares, H.; DeVirgilio, C.; Valle, G.; Chuang, J. S.; Pringle, J. J. *Cell Biol.* **1997**, *139*, 75.

(17) Sloat, B. F.; Pringle, J. R. *Science* **1978**, *200*, 1171.

(18) Dengis, P. B.; Nelissen, L. R.; Rouxhet, P. G. *Appl. Environ. Microbiol.* **1995**, *61*, 718.

(19) Cleveland, J. P.; Manne, S.; Bocek, D.; Hansma, P. K. *Rev. Sci. Instrum.* **1993**, *64*, 403.

(20) Ahimou, F.; Touhami, A.; Dufrene, Y. F. *Yeast* **2003**, *20*, 25.

(21) Koch, Y.; Rademacher, K. H. *Can. J. Microbiol.* **1980**, *26*, 965.

(22) Note that only 10–20% of the cells investigated showed a bud scar. This may be related to the fact that a fraction of the cell population was not in the course of the division process; another possible explanation is that some bud scars may be hidden, i.e., not exposed toward the AFM tip.

(23) Heinz, W. F.; Hoh, J. H. *Tibtech.* **1999**, *17*, 143.

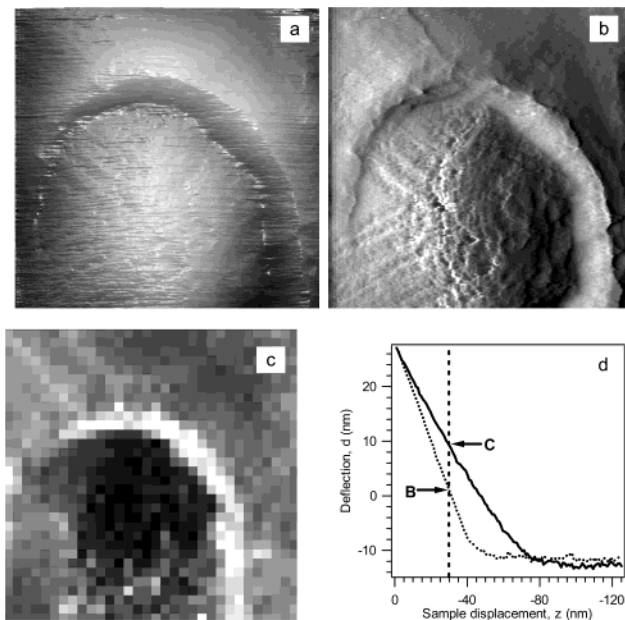


Figure 2. Maps of cell surface topography and mechanical properties. High-resolution height (a) and deflection (b) images ($1.5 \mu\text{m} \times 1.5 \mu\text{m}$) of a portion of the cell showing the bud scar. Force map (c) obtained at the same location by recording a force–volume image consisting of 32×32 force curves and taking a slice of the force volume in the contact region of the curves at a given sample height represented by the vertical dashed line in (d). Differences in gray levels correspond to variations in the deflection magnitude at the selected sample height. In (d), typical curves measured on the mother cell wall (solid line) and on the bud scar (dotted line) are presented and the corresponding deflections are respectively labeled C and B. Similar results were obtained when using different AFM tips and independent cell cultures.

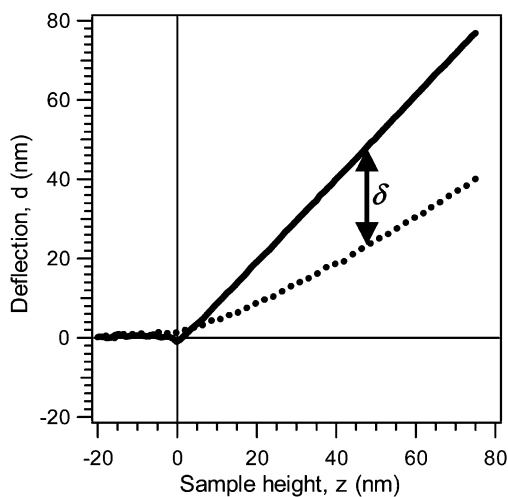


Figure 3. Examples of cantilever deflection versus sample height curves measured on a hard surface, i.e., mica (solid line), and a soft surface, i.e., the yeast cell wall (dotted line). The difference, δ , between both curves is equal to the tip indentation depth.

regions, force curves obtained on both regions were converted into force vs indentation curves and analyzed using the following procedure.^{3,4,6,9}

Figure 3 shows typical raw force curves obtained for hard and soft surfaces, i.e., mica and the yeast surface, respectively. In these curves, the cantilever vertical deflection, d , is plotted as a function of the sample height, z , and the load, F , applied by the cantilever to the tip–

surface contact can be computed using Hooke's law knowing the cantilever spring constant, k_c

$$F = k_c d \quad (1)$$

In the case of mica (Figure 3), the slope of the deflection vs sample height curve was equal to 1 because mica is an infinitely stiff surface compared to the cantilever stiffness. Therefore, this slope was used to calibrate the sensitivity of the position-sensitive photodiode, i.e., to convert the voltage measured on the photodiode into cantilever vertical deflection making the assumption that the tip follows the sample displacement.²⁴ On the soft cell surface, the tip indented the sample surface and the cantilever deflection was smaller than the sample vertical displacement, leading to deflection vs height curves with a slope lower than 1 (Figure 3). The difference between the sample height or cantilever deflection that would be measured on a hard surface and the deflection measured on the soft surface is equal to the indentation depth of the tip into the sample surface, δ

$$\delta = z - d \quad (2)$$

Typical deflection vs sample height curves measured on mica, bud scar, and mother cell wall regions are presented in Figure 4. As can be seen, the deflection of the free cantilever was not equal to zero, due to drift in the detection system as well as to stresses in the cantilever. Therefore, it was necessary to subtract the deflection offset, d_0 , from all the deflection values, this offset being easily determined from the force curve by measuring the average cantilever deflection when the cantilever is far from the sample surface (Figure 4). Then eq 1 was modified in order to evaluate the actual load applied on the contact:

$$F = k_c(d - d_0) \quad (3)$$

To calculate the tip indentation depth, δ (relation 2), the point of contact or height offset, z_0 , where the tip first enters in contact with the sample surface was determined. For typical force curves as measured on mica (Figure 4a), a sudden jump to contact was observed upon approach and the height offset, z_0 , was easily determined as the height where this instability occurs.²⁵ For the bud scar and mother cell regions (Figure 4b,c), this instability was not observed. The determination of the height offset was thus more difficult. In this case, z_0 was defined as the height where the cantilever deflection begins to level off from the horizontal line representing the average deflection when the tip is off-contact, i.e., the deflection offset. Following determination of d_0 and z_0 , the tip indentation depth or tip to surface distance was calculated using relation 2 modified as follows:

$$\delta = (z - z_0) - (d - d_0) \quad (4)$$

Using then eqs 3 and 4, deflection versus height curves were transformed into load, F , versus indentation, δ , curves. Typical F vs δ curves obtained for the bud scar and mother cell regions are shown in Figure 5. These were clearly different, the indentation depth at a given load being much smaller on the bud scar compared to the mother cell surface.

(24) D'Costa, N. P.; Hoh, J. H. *Rev. Sci. Instrum.* **1995**, *66*, 5096.

(25) Burnham, N. A.; Colton, R. J. In *Scanning Tunneling Microscopy and Spectroscopy Theory, Techniques, and Applications*; Bonnell, D. A., Ed.; Springer: New York, 1993; p 191.

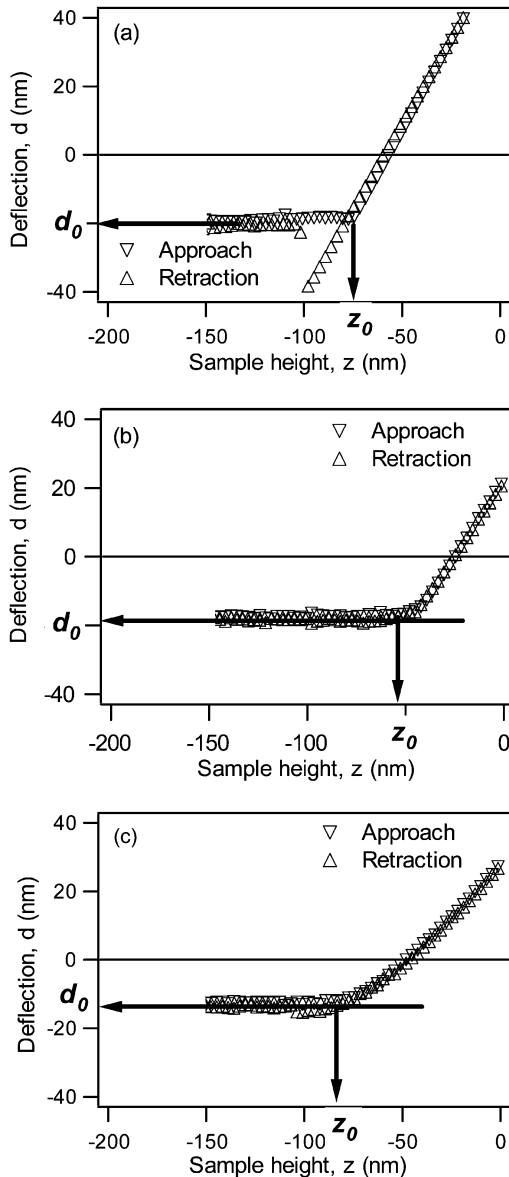


Figure 4. Typical cantilever deflection versus sample height curves obtained on mica (a), on the bud scar (b), and on the mother cell surface (c). The height and deflection offsets are represented by z_0 and d_0 , respectively. Similar curves were obtained when probing different locations of the same regions as well as when using different AFM tips and independent cell cultures.

Young's Modulus. To extract quantitative values of Young's modulus from the force-indentation curves, these were analyzed with Hertzian models from the continuum mechanics of contacts.^{26,27} These simple models are valid for elastic surfaces and do not take into account tip-surface adhesion. Since adhesion forces were always small or negligible in this study, it was reasonable to use these models.²⁸ Hertzian models describe the indentation of a non-deformable indenter (the AFM tip made of silicon or silicon nitride) into an infinitely extending deformable elastic half space (the sample surface). In the case of AFM, the tip shape can be generally modeled by two geometries, a conical or a paraboloid indenter. In these

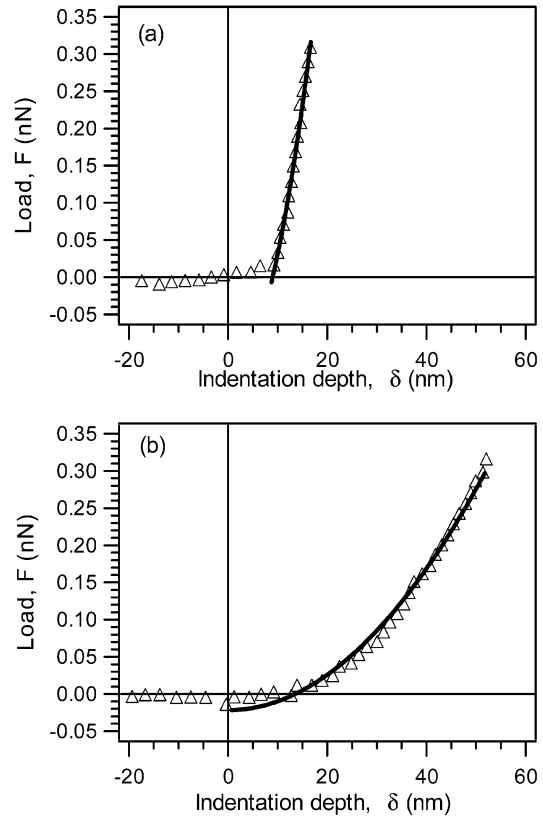


Figure 5. Typical load-indentation curves obtained for the bud scar (a) and surrounding mother cell surface (b). The curves were fitted with the Hertz model (solid lines), yielding Young's modulus values of 6.1 ± 2.4 and 0.6 ± 0.4 MPa for the bud scar and the mother cell surface, respectively (mean values obtained from nine curves from two independent experiments).

cases, the load vs indentation depth relation are respectively given by

$$F_{\text{cone}} = \frac{2}{\pi} \tan \alpha E^* \delta^2 \quad (5)$$

$$F_{\text{paraboloid}} = \frac{4}{3} E^* R^{1/2} \delta^{3/2} \quad (6)$$

In these relations, α is the half-opening angle of a conical tip, R is the radius of curvature of a spherical or paraboloid indenter, and E^* is the surface elastic constant of the material constituting the elastic half space. It is defined by the following equation

$$E^* = \frac{E}{1 - \nu^2} \quad (7)$$

where E is the Young's modulus or tensile elastic modulus of the materials and ν is its Poisson's ratio.

From relations 5 and 6, one can see that if a quasi-quadratic relation is observed between the load and the indentation depth, a conical model should be used for the tip, while if the load versus indentation depth relation is close to a $\delta^{3/2}$ variation, the spherical or paraboloid model should be used. For both the bud scar and mother cell surfaces, quasi-quadratic load-indentation relations were obtained. Therefore, the curves were fitted using the conical model (relation 5) using a value of 18° for the half-opening angle (value given by the manufacturer). It can be seen in Figure 5, that the retraction curves were well fitted by the theoretical model. From these fits and assuming a Poisson's ratio of 0.5, which is expected for

(26) Hertz, H. *J. Reine Angew. Math.* **1882**, *92*, 156.

(27) Sneddon, I. N. *Int. J. Eng. Sci.* **1965**, *3*, 47.

(28) Note that on samples exhibiting significant adhesion forces, it would be more appropriate to use the JKR model: Johnson, K. L.; Kendall, K.; Roberts, A. D. *Proc. R. Soc. London, Ser. A* **1971**, *324*, 301.

soft biological materials, we deduced Young's modulus values of 6.1 ± 2.4 MPa ($n = 9$) for the bud scar and 0.6 ± 0.4 MPa ($n = 9$) for the mother cell surface. The rather large standard deviation on the obtained average values reflects variability of the measurements across the surface of the same cell as well as variability associated with independent cell cultures. From the Young's modulus values, it can be concluded that the bud scar is about 10 times stiffer than the mother cell surface, a finding which is consistent with the presence of chitin in the bud scar.^{16,17}

It is interesting to compare our data to those reported for other cellular systems. We note that our Young's modulus values are significantly larger than those obtained on animal cells (typically, in the 100 Pa to 0.1 MPa range) using similar nanoindentation measurements (see ref 9 for a recent review). This is consistent with differences in cell surface architecture; i.e., thick cell walls are not found in animal cells. Interestingly, the Young's modulus values obtained here are smaller than those reported for other microbial systems. However, there are several reasons why these experiments should not be directly compared. First, some studies dealt with pure, isolated cell wall layers, yielding elastic moduli in the 10 MPa to 10 GPa range.^{11,12} The authors focused on specific proteinaceous and peptidoglycan layers known to have unusual strength, which is very different from the complex, multilayered architecture of the yeast walls. Second, cell wall elasticity has also been measured on whole cells, using micromanipulation²⁹ and optical trapping³⁰ methods. The measurements yielded elastic moduli of 110 and 50 MPa, for *S. cerevisiae* and *Bacillus subtilis*, respectively.

Here, the entire cells were subjected to mechanical stress, which is not the case in local AFM nanoindentation measurements. Clearly, further quantitative comparison of global and local measurements is needed to get a complete picture of the yeast cell wall elasticity.

Summarizing, by use of combined AFM imaging and nanoindentation measurements, regions of different elasticity were distinguished on single yeast cells, in relation with the cell budding process. Fitting force vs indentation curves with the Hertz model yielded a Young's modulus that was about 10 times higher on the bud scar than on the surrounding cell wall. This marked difference in local elasticity was attributed to the accumulation of chitin in the bud scar region during cell division.

Acknowledgment. B.N. and Y.F.D. are Research Associates of the Belgian National Foundation for Scientific Research (FNRS). The support of the FNRS, the Interuniversity Poles of Attraction Program (Federal Office for Scientific, Technical and Cultural Affairs), and of the Research Department of Communauté Française de Belgique (Concerted Research Action) is gratefully acknowledged. The authors thank Professor P. Grange for the use of the AFM and F. Ahimou and S. Derclaye for helping with the experiments.

LA034136X

(29) Smith, A. E.; Zhang, Z. B.; Thomas, C. R.; Moxham, K. E.; Middelberg, A. P. J. *Proc. Natl. Acad. Sci. U.S.A.* **2000**, *97*, 9871.

(30) Mendelson, N. H.; Sarlls, J. E.; Wolgemuth, C. W.; Goldstein, R. E. *Phys. Rev. Lett.* **2000**, *84*, 1627.